Available online at www.sciencedirect.com

SciVerse ScienceDirect

Ceramics International 38 (2012) 2823–2827

CERAMICS INTERNATIONAL

www.elsevier.com/locate/ceramint

Morphotropic phase boundary in the BNT–BT–BKT system

Jean-François Trelcat [a,*], Christian Courtois [a], Mohamed Rguiti [a], Anne Leriche [a], Paul-Henri Duvigneaud [b], Tiriana Segato [b]

[a] *Laboratoire des Matériaux Céramiques et Procédés Associés, EA 2443, Université de Lille Nord de France, PECMA Z.I. Champ de l'Abbesse, Maubeuge, France*

[b] *Service "Matières et Matériaux", Faculté des Sciences Appliquées, Université Libre de Bruxelles, CP165/63 Bruxelles, Belgium*

Received 7 November 2011; accepted 18 November 2011
Available online 28 November 2011

Abstract

Lead-free x $Bi_{0.5}Na_{0.5}TiO_3$–y $BaTiO_3$–z $Bi_{0.5}K_{0.5}TiO_3$ piezoelectric ceramics were synthesized by a conventional solid state reaction method. The microstructure, ferroelectric and piezoelectric properties of the ceramics were investigated. Structure measurements by X-ray diffraction with Rietveld refinement have allowed us to specify more precisely the morphotropic phase boundary (MPB) in this system. For $(1-x)$ BNT–x BT solid solution ceramics, the 0.94 BNT–0.06 BT morphotropic composition shows the higher values with d_{33} = 170 pC/N, k_p = 0.35 and k_t = 0.53. In the case of $(1-x)$ BNT–x BKT compositions, the d_{33}, k_p and k_t are, respectively, 137 pC/N, 0.39 and 0.54 for the 0.80 BNT–0.20 BKT ceramic. On the other hand, the ternary 0.865 BNT–0.035 BT–0.100 BKT morphotropic composition shows high piezoelectric constant and electromechanical coupling factors (d_{33} = 133 pC/N, k_p = 0.26 and k_t = 0.57).

Keywords: C. Electrical properties; C. Piezoelectric properties; Lead-free; Piezoelectric ceramics; Morphotropic phase boundary; Solid state reaction; Bismuth sodium titanate; Bismuth potassium titanate; Barium titanate

1. Introduction

Piezoelectric ceramics based on lead, titanium and zirconium oxides in a perovskite like structure (PZT) present the most interesting piezoelectric properties near the morphotropic phase boundary and are used in many electronic and ultrasonic applications (sensors, actuators and transformers [1–3]). However, due to the effects of lead toxicity, considerable efforts were made recently to develop lead-free piezoelectric ceramics. According to 2002/95/EC and 2002/96/EC directives [4], the exclusion of electronic part including lead compounds is restricted gradually and will be prohibited in a near future.

Unfortunately, alternative lead free materials do not exhibit the same piezoelectric characteristics of PZT. Numerous works turn towards new promising lead free materials to improve their piezoelectric properties in order to progressively replace PZT devices. The most studied materials are $KNbO_3$, $K_xNa_{1-x}NbO_3$, $LiNbO_3$, $LiNa_{1-x}NbO_3$ and $Bi_{0.5}Na_{0.5}TiO_3$-based systems [5].

This study focuses on the $Bi_{0.5}Na_{0.5}TiO_3$–$BaTiO_3$–$Bi_{0.5}K_{0.5}TiO_3$ system. This system is composed of three perovskite phases. As the other piezoelectric materials, the better properties are expected near the rhombohedral–tetragonal morphotropic phase boundary.

Literature shows that this zone is not well defined in composition [6,7] and more works are needed to determine more precisely this boundary. In this paper, several compositions in the $Bi_{0.5}Na_{0.5}TiO_3$–$BaTiO_3$–$Bi_{0.5}K_{0.5}TiO_3$ system have been studied in order to determine the morphotropic boundary.

Previous works reported promising piezoelectric properties for mixed $(1-x)$ BNT–x BT compositions with x values between 0.06 and 0.08 [8] and for $(1-x)$ BNT–x BKT with x values between 0.16 and 0.20 [9]. Fig. 1 shows the empirical BNT–BT–BKT ternary phase diagram proposed by literature [10,11].

2. Experimental

The studied compositions in this work are listed in Table 1. In the first series of samples concerning binary $(1-x)$ BNT–x BT system, the x value is increased from 0 to 0.07. The second

* Corresponding author.
E-mail address: jeanfrancois_trelcat@yahoo.fr (J.-F. Trelcat).

0272-8842/$36.00
doi:10.1016/j.ceramint.2011.11.053

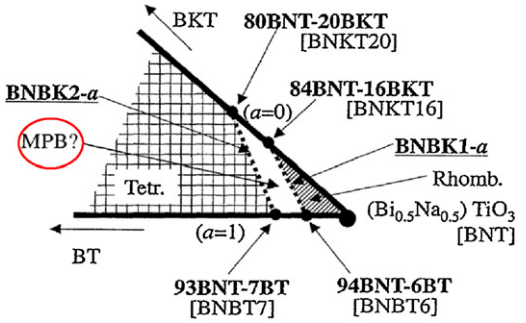

Fig. 1. Empirical phase diagram of BNT–BT–BKT system [10,11].

series of samples lies in the binary $(1-x)$ BNT–x BKT system with x varying from 0 to 0.20. Three compositions constitute the third series and are located in the predicted morphotropic area of the ternary BNT–BT–BKT system.

The materials are synthesized by the conventional solid state reaction method from mixed oxides (TiO_2 and Bi_2O_3) and carbonates ($BaCO_3$, $NaCO_3$ and K_2CO_3). Starting from 0.1 mole of TiO_2, other precursors are weighed in order to obtain several compositions in the ternary diagram $Bi_{0.5}Na_{0.5}$-TiO_3–$BaTiO_3$–$Bi_{0.5}K_{0.5}TiO_3$. The different used powders are of purity over 99.9%. The powders are mixed and ground in a planetary mill during 30 min at 300 rpm with ethanol and dried at 60 °C. A first thermal treatment at 825 °C during 4 h is carried out to eliminate carbonates and initiate the chemical reactions. After calcining, the ground powders were isostatic pressed. The sintering was carried out at 1150 °C during 4 h in air. These conditions have been chosen in order to avoid any vaporisation of Bi and K elements. The as-prepared samples consist of disks of 15 mm in diameter and 1.5 mm in thickness. The samples were examined with several techniques. The microstructure was observed by scanning electron microscopy (SEM) after chemical etching. The theoretical density for each composition was calculated using the law of mixture and the densities of $Bi_{0.5}Na_{0.5}TiO_3$, $BaTiO_3$ and $Bi_{0.5}K_{0.5}TiO_3$ pure phases, respectively, 5.99 g/cm^3 (ICDD n°36-0340), 6.01 g/cm^3 (ICDD n°05-0626) and 5.93 g/cm^3 (ICDD n°36-0339). The relative density was obtained after measuring the external dimensions and weighing and was compared with the theoretical one. Sample compositions were determined by X-ray fluorescence and the crystallisation state was investigated by X-ray diffraction. For electrical measurement, silver electrodes were deposited by screen printing on each faces. The silver paste was dried at 150 °C during 15 min and fired at 650 °C during 5 min. The electric field applied for polarisation varied between 3 and 6 kV/mm. The polarisation step was operated in an oil bath heated to 60 °C during 1 h. A piezometer (PIEZOTEST, Piezometer system PM200) was used to measure the charge constant d_{33}. The resonance and anti-resonance frequencies f_r and f_a obtained on polar and thickness modes, the capacity C_p, the dissipation factor $\tan\delta$ and the minimum impedance Z_m were measured with an impedance analyser (HP4194A, 100 Hz to 40 MHz). Starting from the as-obtained values, the dielectric constant ε_r, the mechanical quality factor Q_m and the electromechanical coupling factors k_t and k_p were calculated with the following equations:

$$\varepsilon_r = \frac{(C_p \times e)}{(\varepsilon_0 \times S)}$$

$$Q_m = \frac{f_a^2}{\{2\pi \times f_r \times Z_m \times C_p \times (f_a^2 - f_r^2)\}}$$

$$k_p^2 = 2.51 \times \left\{\frac{(f_a - f_r)}{f_a}\right\} - \left\{\frac{(f_a - f_r)}{f_a}\right\}^2$$

$$k_t^2 = \frac{\{(\pi/2) \times (f_r - f_a)\}}{\tan\{(\pi/2) \times (f_r - f_a)\}}$$

with ε_0, e and S are, respectively, the vacuum permittivity, the thickness and the surface of samples.

Table 1
Studied compositions.

Compounds
BNT
0.96 BNT–0.04 BT
0.94 BNT–0.06 BT
0.935 BNT–0.065 BT
0.93 BNT–0.07 BT
0.88 BNT–0.12 BKT
0.84 BNT–0.16 BKT
0.80 BNT–0.20 BKT
0.865 BNT–0.035 BT–0.100 BKT
0.892 BNT–0.054 BT–0.054 BKT
0.89 BNT–0.03 BT–0.08 BKT

3. Results and discussions

Theoretical and relative densities for the different studied samples are plotted in Table 2. A relative density of 92–95% is reached for all the samples.

These high density values are confirmed by SEM observation. Fig. 2 shows the microstructure of the 0.865 BNT–0.035 BT–0.100 BKT ceramic. The grain size is ranging between 0.2 μm and 1 μm.

The composition of the various samples was verified after sintering by X-ray fluorescence in order to check whether volatilisation has occurred. As example, Table 3 presents oxide contents before and after sintering for three compositions: 0.94 BNT–0.06 BT, 0.80 BNT–0.20 BKT and 0.865 BNT–0.035 BT–0.100 BKT. Compositions after sintering are close to the target ones and no loss of volatile elements occurs in these sintering conditions.

X-ray diffraction measurements show that all the sintering samples present a tetragonal or rhombohedral structure or a mixture of these both phases. Fig. 3 shows the rhombohedral–tetragonal transition through three compositions: 0.94 BNT–0.06 BT, 0.935 BNT–0.065 BT and 0.93 BNT–0.07 BT.

The rhombohedral structure is characterized by a (0 0 3)/(0 2 1) peak splitting between 39 and 41° and a (1 0 4)/(1 2 2) peak splitting between 57 and 59° whereas a pure tetragonal

Table 2
Compositions, theoretical density and relative density after sintering.

Compounds	Theoretical density (g/cm^3)	Density after sintering (g/cm^3)	Relative density (%)
BNT	5.99	5.62	94
0.96 BNT–0.04 BT	5.99	5.61	94
0.94 BNT–0.06 BT	5.99	5.58	93
0.935 BNT–0.065 BT	5.99	5.49	92
0.93 BNT–0.07 BT	5.99	5.67	95
0.88 BNT–0.12 BKT	5.98	5.60	94
0.84 BNT–0.16 BKT	5.98	5.51	92
0.80 BNT–0.20 BKT	5.97	5.66	95
0.865 BNT–0.035 BT–0.100 BKT	5.98	5.65	94
0.892 BNT–0.054 BT–0.054 BKT	5.98	5.69	95
0.89 BNT–0.03 BT–0.08 BKT	5.98	5.50	92

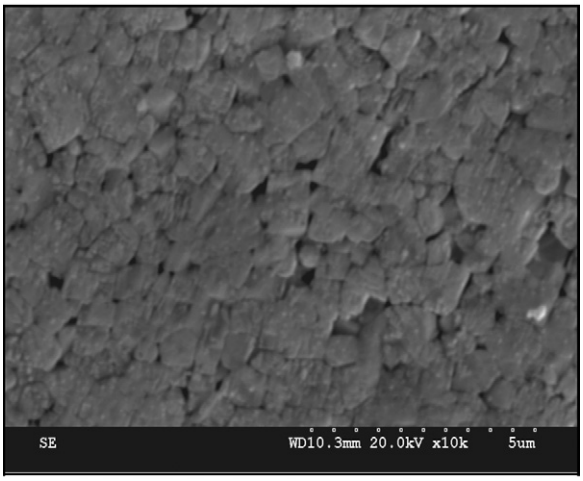

Fig. 2. SEM observation of 0.865 BNT–0.035 BT–0.100 BKT.

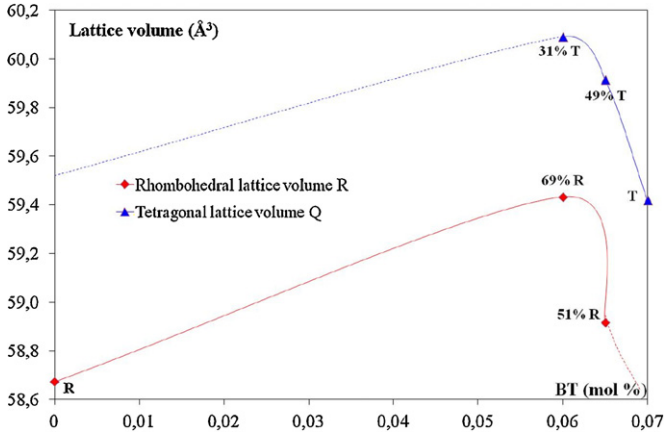

Fig. 4. Equivalent lattice volume dependence of BT molar ratio. (For interpretation of the references to color in text, the reader is referred to the web version of the article.)

structure is characterized by a single peak (1 1 1) at 40° and a single peak corresponding to two crystal planes (1 1 2) and (2 1 1) at 57.7°. The proportions of each phase and the equivalent rhombohedral and tetragonal lattice volumes have been determined by means of Rietveld refinement. Fig. 4 shows

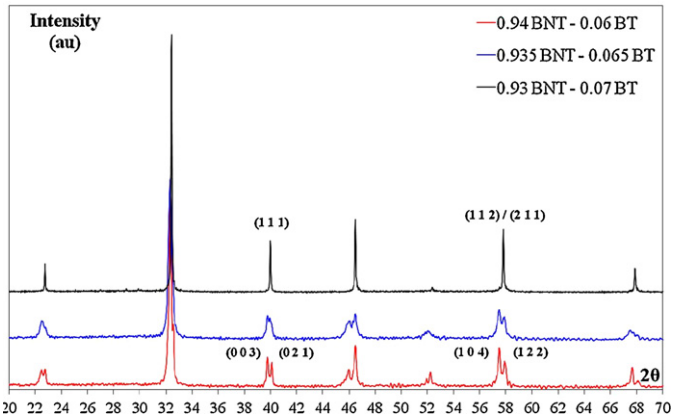

Fig. 3. X-ray diffraction of 0.94 BNT–0.06 BT; 0.935 BNT–0.065 BT and 0.93 BNT–0.07 BT.

Table 3
Sample compositions before and after sintering (wt.%) for 0.94 BNT–0.06 BT; 0.80 BNT–0.20 BKT and 0.865 BNT–0.035 BT–0.100 BKT.

Equivalent oxides	Initial composition (wt.%)	After sintering (wt.%)
TiO_2	37.46	37.42
Bi_2O_3	51.37	51.34
BaO	4.31	4.25
Na_2O	6.83	6.80
0.94 BNT–0.06 BT		
TiO_2	37.38	37.35
Bi_2O_3	54.56	54.54
Na_2O	5.81	5.79
K_2O	2.19	2.18
0.80 BNT–0.20 BKT		
TiO_2	37.42	37.29
Bi_2O_3	52.68	52.58
BaO	2.52	2.51
Na_2O	6.28	6.24
K_2O	1.10	1.08
0.865 BNT–0.035 BT–0.100 BKT		

Table 4
Samples electrical properties and volume % of phases determined after Rietveld refinement.

Compounds	ε_r	Tan δ (%)	d_{33} (pC/N)	k_p	k_t	T/R
BNT	423	5.0	67 ± 10	0.11 ± 0.01	0.49 ± 0.02	0/100
0.96 BNT–0.04 BT	532	1.7	123 ± 10	0.13 ± 0.01	0.43 ± 0.02	0/100
0.94 BNT–0.06 BT	***782***	***3.1***	***170 ± 4***	***0.35 ± 0.02***	***0.53 ± 0.05***	***31/69***
0.935 BNT–0.065 BT	***873***	***3.4***	***147 ± 9***	***0.26 ± 0.01***	***0.49 ± 0.05***	***49/51***
0.93 BNT–0.07 BT	626	2.1	123 ± 3	0.18 ± 0.02	0.45 ± 0.05	100/0
0.88 BNT–0.12 BKT	541	4.1	78 ± 9	0.22 ± 0.01	0.43 ± 0.03	24/76
0.84 BNT–0.16 BKT	***710***	***3.6***	***130 ± 7***	***0.29 ± 0.01***	***0.44 ± 0.02***	***100/0***
0.80 BNT–0.20 BKT	***936***	***3.9***	***137 ± 7***	***0.39 ± 0.01***	***0.54 ± 0.05***	***100/0***
0.892 BNT–0.054 BT–0.054 BKT	***904***	***3.6***	***130 ± 10***	***0.20 ± 0.02***	***0.43 ± 0.01***	***65/35***
0.89 BNT–0.03 BT–0.08 BKT	665	3.8	112 ± 4	0.26 ± 0.01	0.44 ± 0.02	40/60
0.865 BNT–0.035 BT–0.100 BKT	***891***	***4.2***	***133 ± 6***	***0.26 ± 0.02***	***0.57 ± 0.05***	***>90/<10***

the evolution of equivalent lattice volume according to the increase of the BT molar ratio for the binary $(1-x)$ BNT–x BT.

The 0.93 BNT–0.07 BT composition shows a pure tetragonal pattern. The 0.935 BNT–0.065 BNT composition is a 51% rhombohedral and 49% tetragonal mixture showing a peak shift towards small angle due to the barium substitution for sodium and an increase of tetragonal peak intensity. For $x > 0.065$, a hypothesis can be advanced: the average phase mixture volume has to remain logically constant (the morphotropic boundary takes place in the solid state). Thus, the rhombohedral phase volume decreases to balance the tetragonal phase volume decreasing, explaining the proposed extrapolations (in red dotted line in Fig. 4). The same reasoning can be proposed for $x < 0.060$ (in blue dotted line in Fig. 4).

Table 4 summarises the proportion of each phase and electrical properties measured for the different compositions. The maximum poling electrical field applied is 6 kV/mm. The value of this poling field is low compared to other values found in literature [12], but higher poling field values induced cracking samples. Regarding the binary BKT–BNT, a transition is observed between 12% (24% tetragonal) and 16% of BKT (100% tetragonal). All the ternary compositions present mixed tetragonal–rhombohedral phases in different proportions.

From these results, new morphotropic boundary limits on the ternary diagram are proposed. The morphotropic boundary is then likely in the area delimited by the two red lines (Fig. 5). This result shows that the morphotropic area is larger than proposed by literature [10,11] and shifted towards less BKT amounts.

For all compositions, the dielectric constant increases with the BT or BKT amount increasing. The maximum value is obtained for the 0.80 BNT–0.20 BKT composition with $\varepsilon_r = 936$. Compared with the pure BNT sample, the dissipation factor obtained for all binary or ternary compositions is globally lower (between 1.7 and 4.2%).

The charge constant d_{33} as well as the k_p values of the samples are reported in the ternary diagram (Fig. 7). The charge constant d_{33} and k_p reach maximum values for the 0.060 and 0.065 BT contents on the BNT–BT axis which exhibit the two phases (Fig. 6). Both compositions exhibit a mixture rhombohedral–tetragonal phases.

The 0.88 BNT–0.12 BKT composition which contains only 24% tetragonal phase presents the lowest d_{33} value (78 pC/N) in BNT–BKT binary compositions.

The two compositions 0.80 and 0.84 of BNT exhibit higher value for d_{33} despite the occurrence of the only tetragonal peaks

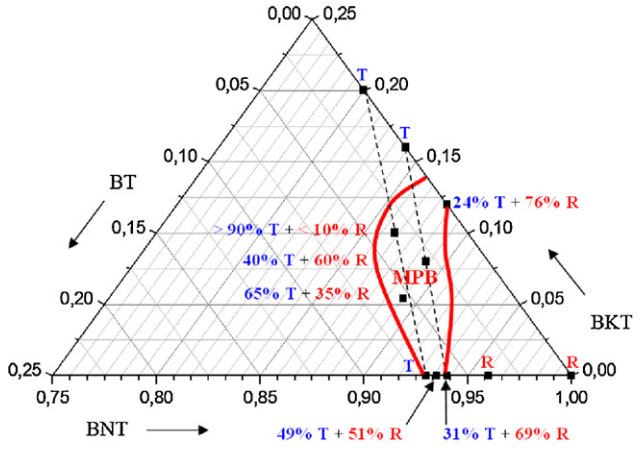

Fig. 5. MPB as observed (in red lines) and compared to literature (in dotted black lines) [10,11]. (For interpretation of the references to color in this figure legend, the reader is referred to the web version of the article.)

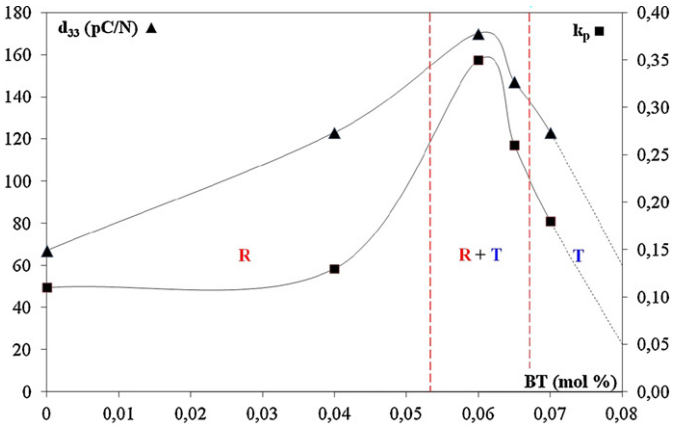

Fig. 6. d_{33} and k_p values observed on BNT–BT axis near the morphotropic transition.

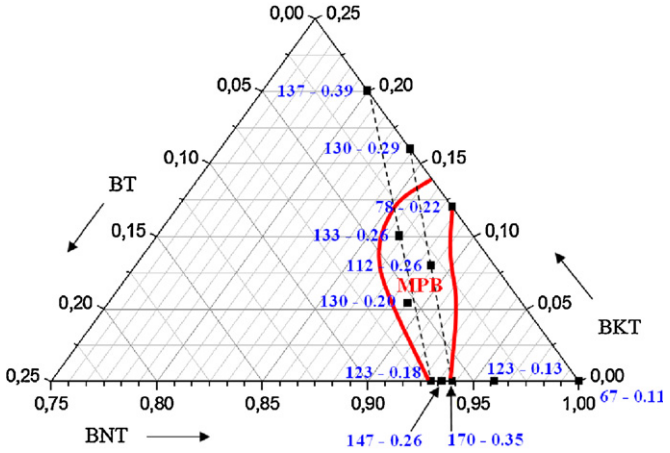

Fig. 7. d_{33} and k_p values observed on the ternary diagram.

which should suggest that they are very close to the morphotropic area boundary.

For the ternary mixed compositions, the charge constant varies around 120–130 pC/N with a mixture of tetragonal and rhombohedral phases. In contrast, the ternary mixed composition with the lowest amount of BNT is nearly purely tetragonal.

4. Conclusion

BNT–BT–BKT compositions around the morphotropic phase boundary were synthesized from conventional mixed oxide method and their piezoelectric properties were determined. The stoichiometry of the samples after sintering has been confirmed by X-ray fluorescence. All materials present a relative density around 92–95%. X-ray diffraction analysis has shown that all the compositions are characterized by a pure perovskite structure without any parasite phase.

A structural evolution has been confirmed in relation with the composition in the case of $(1 - x)$ BNT–x BT for $x = 0$ to $x = 0.07$. The rhombohedral–tetragonal phase transition occurs between $x = 0.04$ and $x = 0.07$. The best piezoelectrical properties for this system are obtained in the morphotropic area and correspond to $x = 0.06$ and 0.065.

For the $(1 - x)$ BNT–x BKT system, the boundary between the morphotropic area and the tetragonal one is located between $x = 0.12$ and $x = 0.16$.

For the ternary compositions the morphotropic area has been more precisely defined. Two compositions, 0.892 BNT–0.054 BT–0.054 BKT and 0.89 BNT–0.03 BT–0.08 BKT exhibit both the two structures. The third composition 0.865 BNT–0.350 BT–0.100 BKT is nearly pure tetragonal but nevertheless is located at the morphotropic phase boundary which is confirmed by its good piezoelectric values.

Acknowledgment

This work was funded by French Government for a PhD thesis program.

References

[1] S. Matsumoto, A. Klein, R. Maeda, Development of bidirectional valveless micropump for liquid, Procedure of IEEE Micro Electro Mechanical System (1998) 141–146.
[2] A. Schroth, L. Lee, S. Matsumoto, R. Maeda, Application of sol–gel deposited thin PZT film for actuation of 1D and 2D scanners, Sensors and Actuators 73 (1999) 144–152.
[3] J. Chu, Z.J. Wang, R. Maeda, K. Kataota, T. Itih, T. Suga, Novel multibridge-structured piezoelectric microdevices for scanning force microscopy, Journal of Vacuum Science and Technology B18 (2000) 3604–3607.
[4] Directive 2002/95/EC of European Parliament and of the Council of 27 January 2003 on restriction of the use of certain hazardous substances in electrical and electronic equipment, Official Journal of the European Union (2003).
[5] S. Yasuyoshi, T. Hisaaki, T. Tashihiko, N. Tatsukiko, Lead-free piezoceramics, Nature 432 (November) (2004).
[6] Y. Qu, D. Shan, J. Song, Effect of A-site substitution on crystal component and dielectric properties in $Bi_{0.5}Na_{0.5}TiO_3$ ceramics, Materials Sciences and Engineering B121 (2005) 148–151.
[7] C. Peng, J.F. Li, W. Gong, Preparation and properties of $(Bi_{1/2}Na_{1/2})TiO_3$–$Ba(Ti,Zr)O_3$ lead-free piezoelectric ceramics, Materials Letters 59 (2005) 1576–1580.
[8] B.J. Chu, D.R. Chen, G.R. Li, Q.R. Yin, Electrical properties of $Na_{1/2}Bi_{1/2}TiO_3$–$BaTiO_3$ ceramics, Journal of European Ceramic Society 22 (2002) 2115–2121.
[9] A. Sasaky, T. Chiba, Y. Mamiya, E. Otsuki, Dielectric and piezoelectric properties of $(Bi_{0.5}Na_{0.5})TiO_3$–$(Bi_{0.5}K_{0.5})TiO_3$ systems, Japanese Journal of Applied Physics 38 (1999) 5564–5567.
[10] H. Nagata, M. Yoshida, Y. Makiuchi, T. Takenaka, Large piezoelectric constant and high curie temperature of lead-free piezoelectric ceramic ternary system based on bismuth sodium titanate–bismuth potassium titanate–barium tinanate near the morphotropic phase boundary, Japanese Journal of Applied Physics 42 (2003) 7401–7403.
[11] T. Takenaka, H. Nagata, Current status and prospects of lead-free piezoelectric ceramics, Journal of the European Ceramic Society 25 (2005) 2693–2700.
[12] Q. Xu, S. Wu, S. Chen, W. Chen, J. Lee, J. Zhou, H. Sun, Y. Li, Influences of poling condition and sintering temperature on piezoelectric properties of $(Na_{0.5}Bi_{0.5})_{1-x}Ba_xTiO_3$ ceramics, Materials Research Bulletin 40 (2005) 373–382.